Supporting Information

Boosting reaction kinetics and improving long cycle life in lamellar VS_2/MoS_2 Heterojunctions for superior sodium storage performance

Runze Fan[1], Chenyu Zhao[1], Jiahui Ma[1], Shulai Lei[2,*], Guijie Liang[2], Tao He[1], Guocheng Zhu[3], Yurong Cai[1,*]

[1] The Key Laboratory of Advanced Textile Materials and Manufacturing Technology of Ministry of Education, National Engineering Lab for Textile Fiber Materials and Processing Technology, School of Materials Science and Engineering, Zhejiang Sci-Tech University, Hangzhou 310018, China

[2] Hubei Key Laboratory of Low Dimensional Optoelectronic Materials and Devices, Hubei University of Arts and Science, Xiangyang 441053, PR China

[3]College of Textile Science and Engineering (International institute of silk), Zhejiang Sci-Tech University, Hangzhou 310018, China

[*] Corresponding author.

E-mail addresses: sllei@hbuas.edu.cn (Shulai Lei), caiyr@zstu.edu.cn (Yurong Cai).

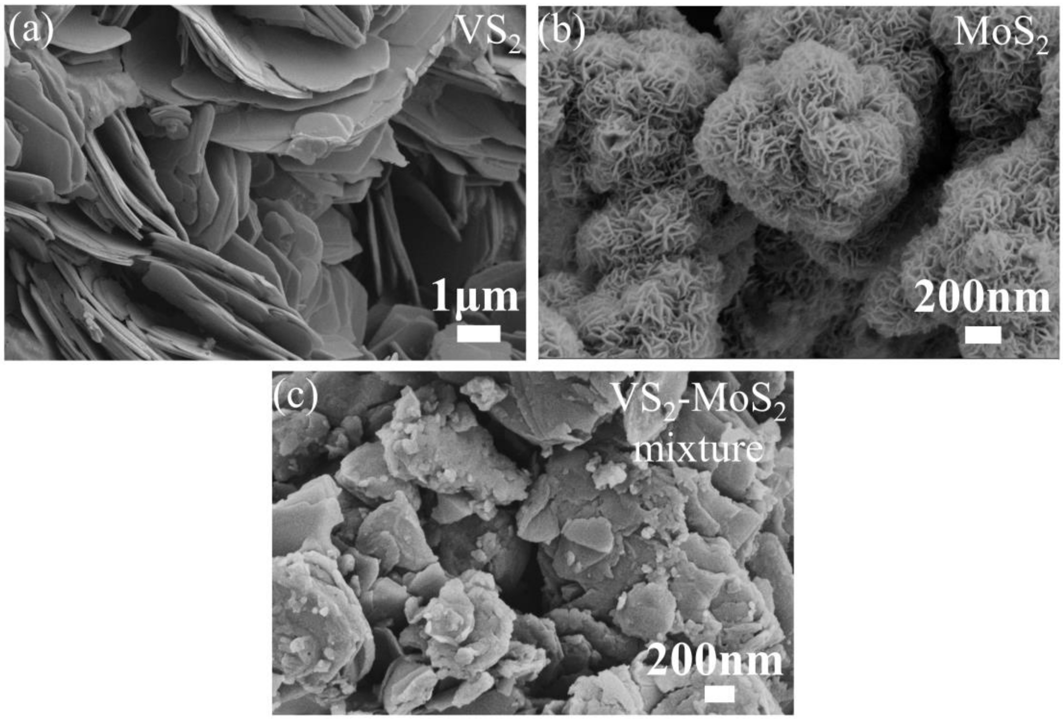

Figure S1. SEM patterns of the a) VS_2, b) MoS_2 and c) VS_2-MoS_2 mixture electrodes.

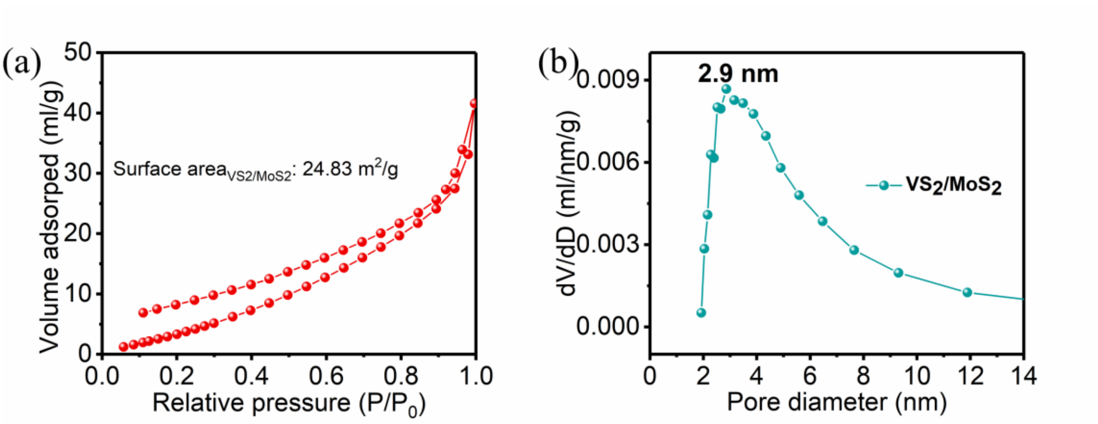

Figure S2. a) N_2 adsorption-desorption isotherms and b) pore size distribution (BJH model) of VS_2/MoS_2.

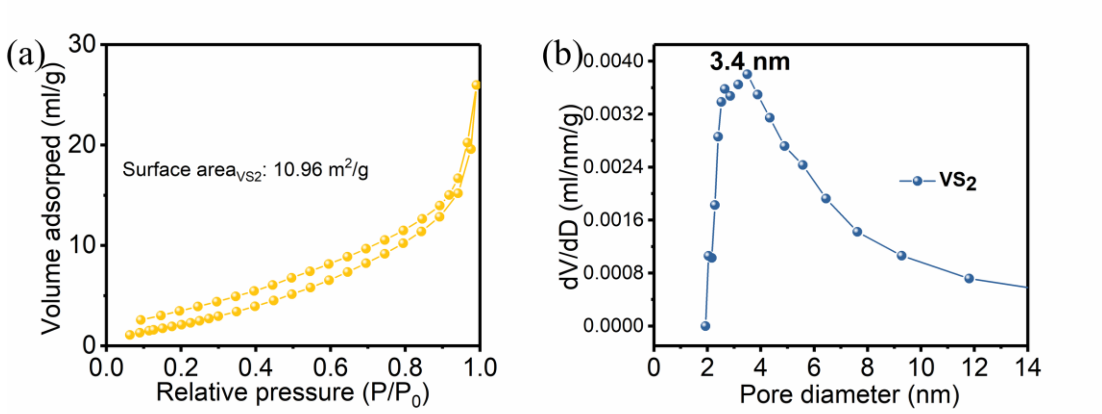

Figure S3. a) N_2 adsorption-desorption isotherms and b) pore size distribution (BJH model) of VS_2.

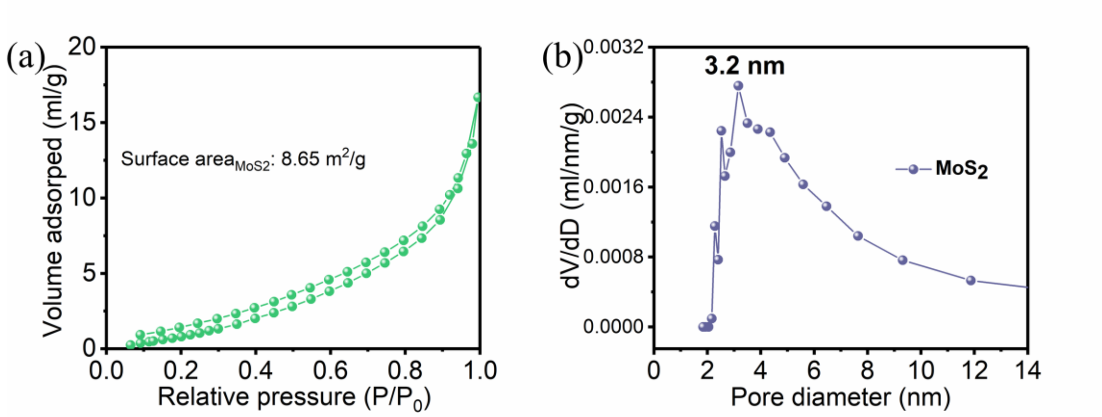

Figure S4. a) N_2 adsorption-desorption isotherms and b) pore size distribution (BJH model) of MoS_2.

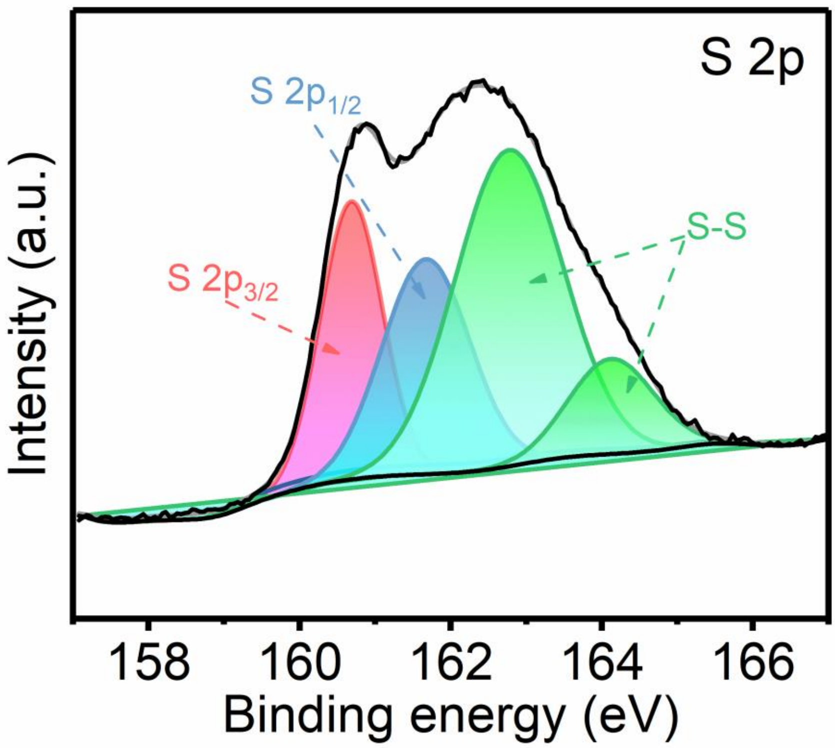

Figure S5. High-resolution XPS spectra of VS_2/MoS_2: S 2p.

The S 2p high-resolution XPS spectrum had two peaks at 160.67eV and 161.66 eV, which were attributed to S $2p_{3/2}$ and S $2p_{1/2}$, respectively. The other two peaks at 162.76 eV and 164.14 eV were ascribed to the supersaturated S-S bonds, which were formed due to the excessive TAA and anchored on the surface of sample. These results indicated that MoS_2 was successfully introduced into VS_2 to form a VS_2/MoS_2 heterostructure.[S1]

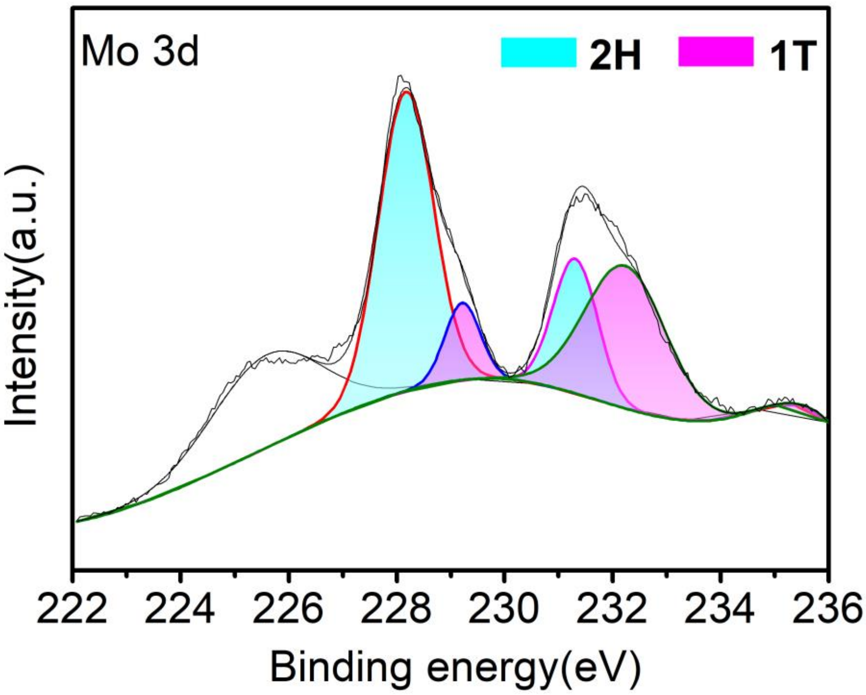

Figure S6. Mo 3d XPS spectra of the VS_2/MoS_2 composite.

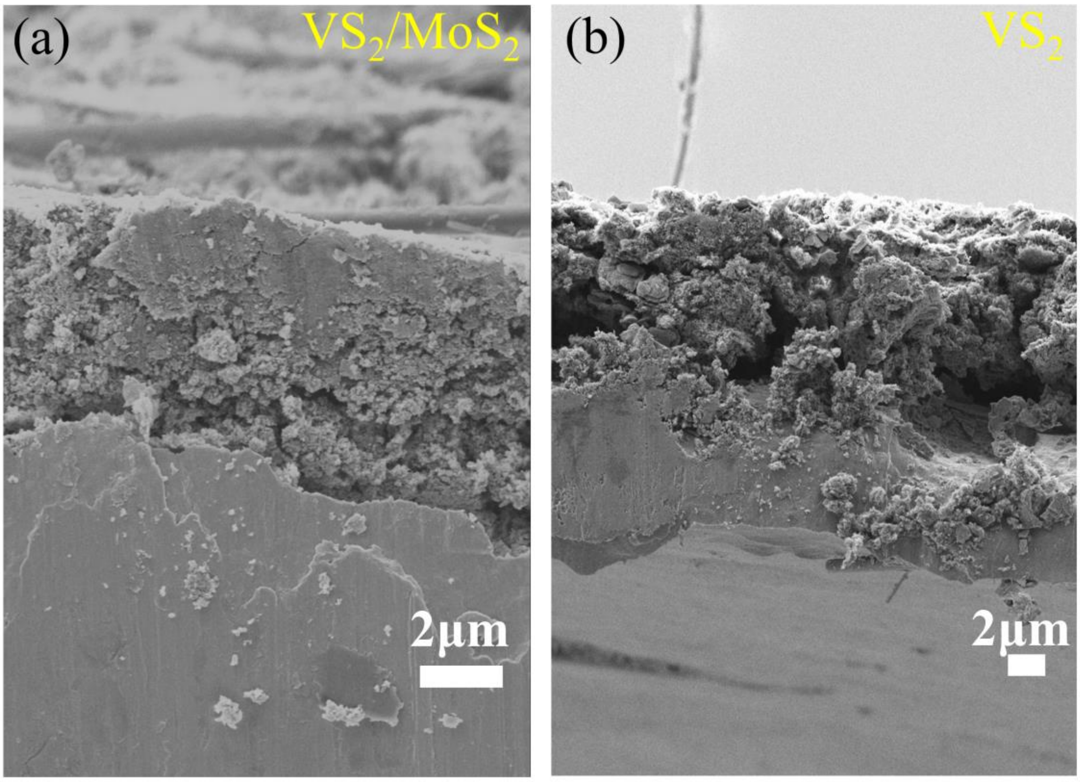

Figure S7. Cross-sectional SEM images of the a) VS_2/MoS_2, b) VS_2 after 100 discharge-charge cycles at 2 A g^{-1}.

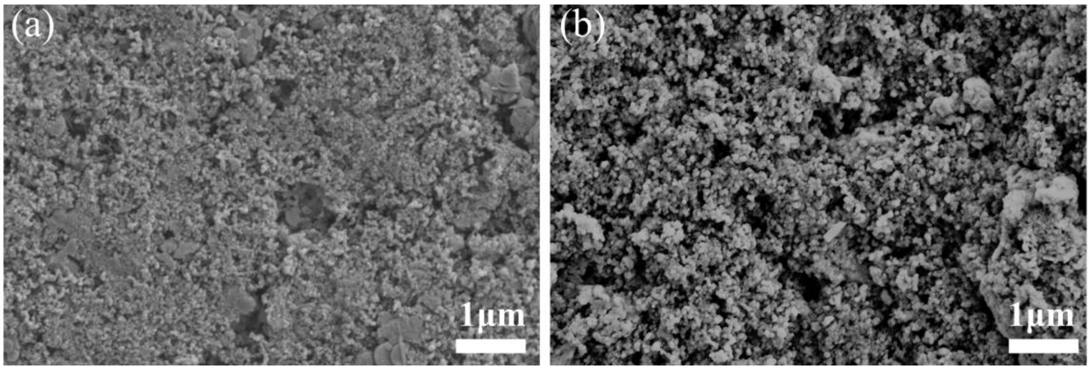

Figure S8. SEM images of VS_2/MoS_2 a) for pristine electrode, b) after 200 discharge-charge cycles at 2 A g^{-1}.

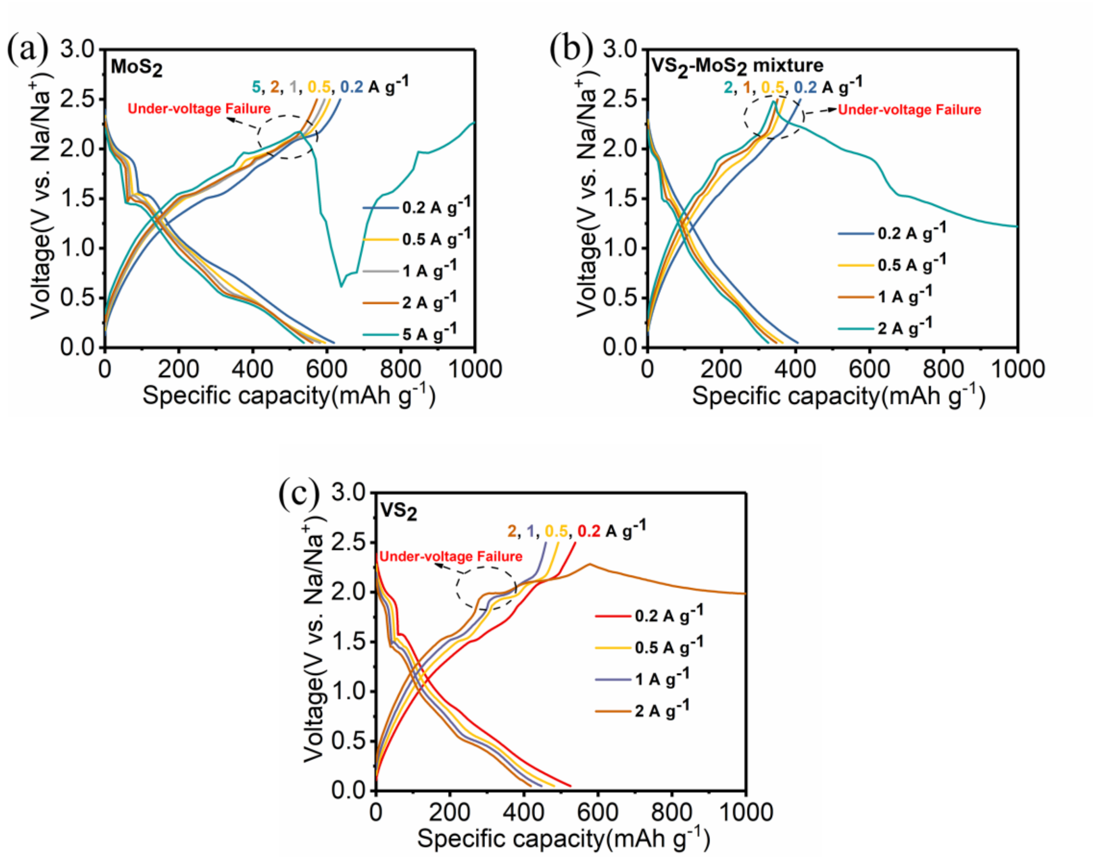

Figure S9. Abnormal discharge/charge patterns of a) MoS_2, b) VS_2-MoS_2 mixture and c) VS_2 anodes at different current densities.

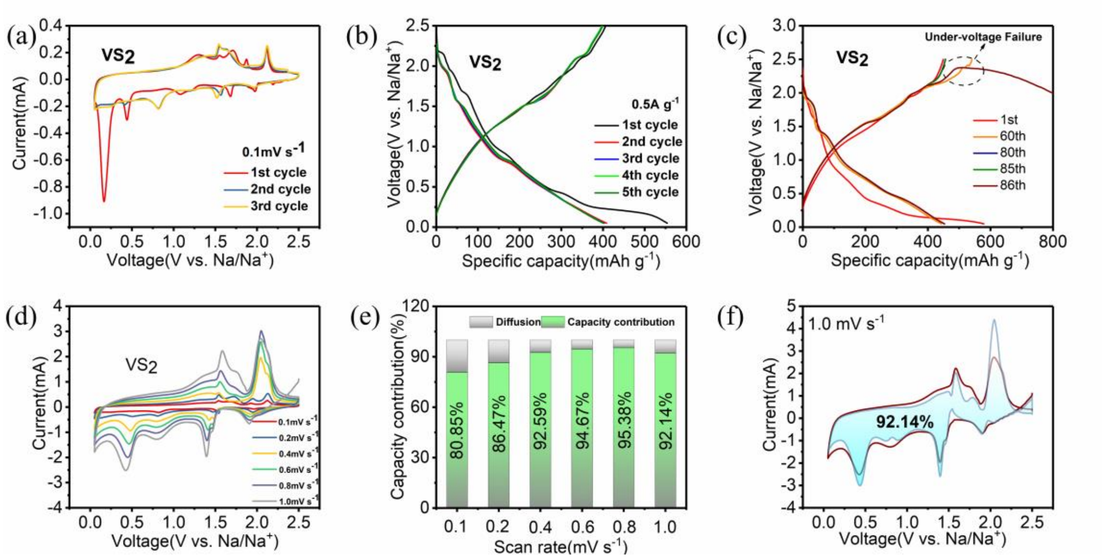

Figure S10. a) CV curves of VS_2 with initial three cycles at 0.1 mV s^{-1}. b) Galvanostatic charge-discharge curves of VS_2 at 0.5 A g^{-1} during the initial five cycles. c) Abnormal galvanostatic discharge/charge patterns of VS_2 anode at 2A g^{-1}. d) CV curves of VS_2 electrode at various scan rates. e) Pseudocapacitive contribution of VS_2 at various scan rates. f) The ratio of diffusion and capacitive contribution to the total capacity at a scan rate of 1 mV s^{-1} for VS_2 electrode.

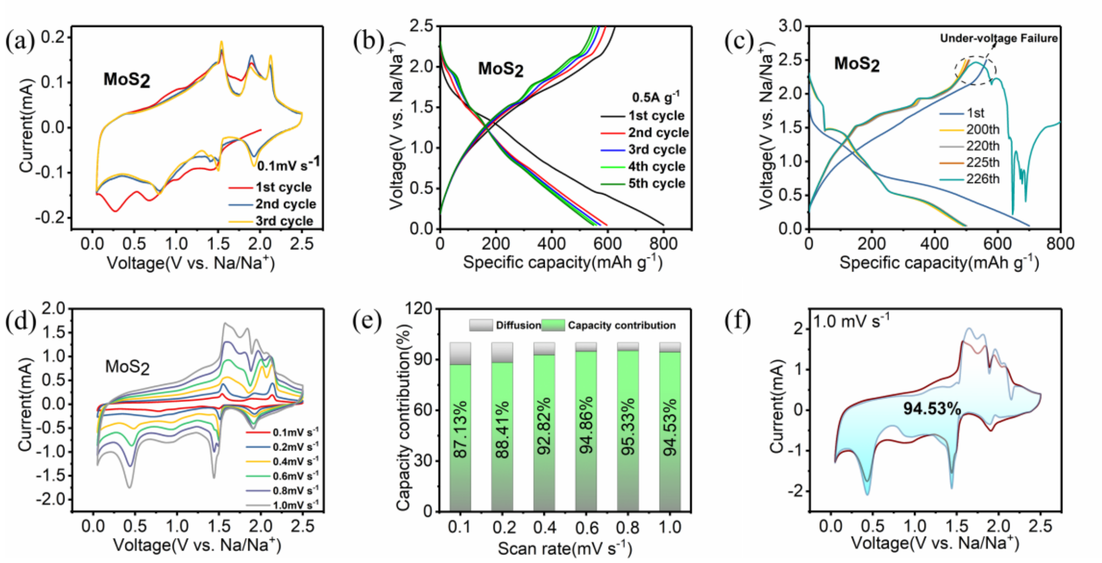

Figure S11. a) CV curves of MoS_2 with initial three cycles at 0.1 mV s^{-1}. b) Galvanostatic charge-discharge curves of MoS_2 at 0.5 A g^{-1} during the initial five cycles.

c) Abnormal galvanostatic discharge/charge patterns of MoS_2 anode at 2A g^{-1}. d) CV curves of MoS_2 electrode at various scan rates. e) Pseudocapacitive contribution of MoS_2 at different scan rates. f) The ratio of diffusion and capacitive contribution to the total capacity at a scan rate of 1 mV s^{-1} for MoS_2 electrode.

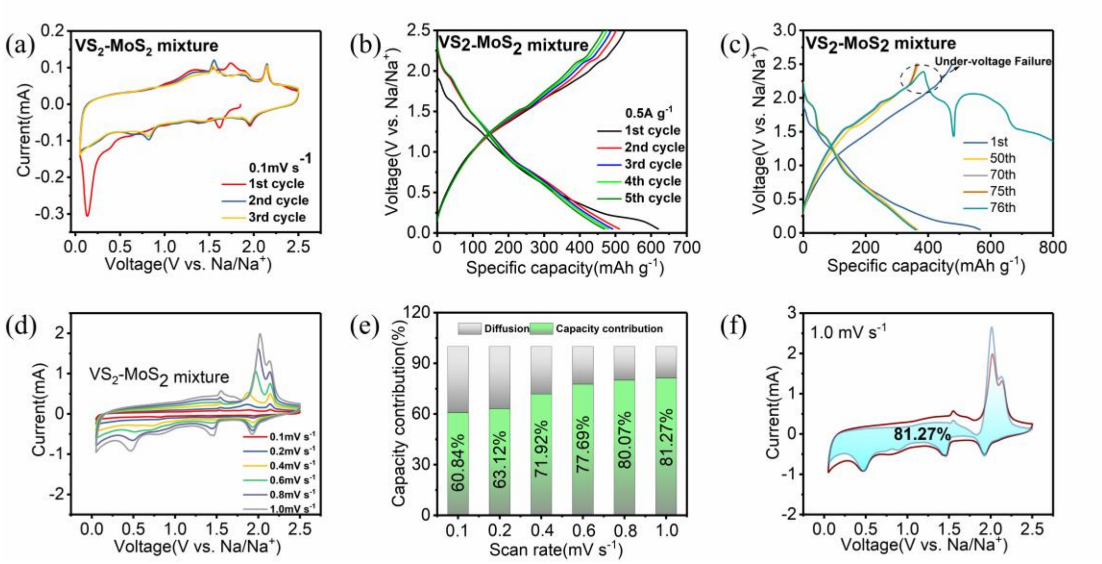

Figure S12. a) CV curves of VS_2-MoS_2 mixture with initial three cycles at 0.1 mV s^{-1}. b) Galvanostatic charge-discharge curves of VS_2-MoS_2 mixture at 0.5 A g^{-1} during the initial five cycles. c) Abnormal galvanostatic discharge/charge patterns of VS_2-MoS_2 mixture anode at 2A g^{-1}. d) CV curves of VS_2-MoS_2 mixture electrode at various scan rates. e) Pseudocapacitive contribution of VS_2-MoS_2 mixture at different scan rates. f) The ratio of diffusion and capacitive contribution to the total capacity at a scan rate of 1 mV s^{-1} for VS_2-MoS_2 mixture electrode.

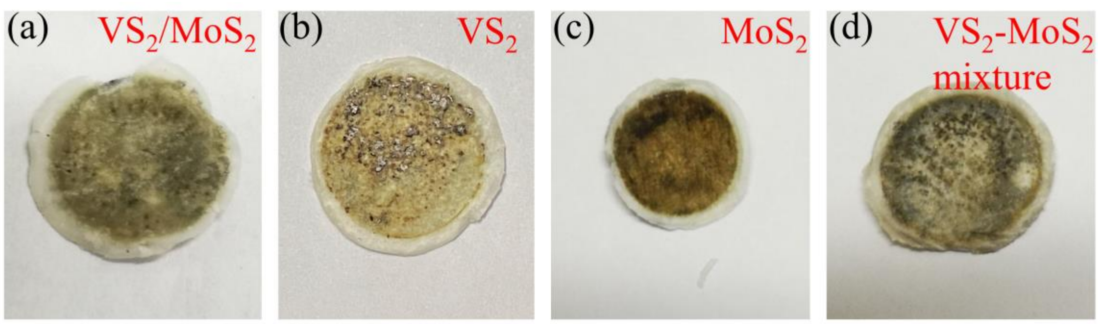

Figure S13. The photos of the separators from the spent a) VS_2/MoS_2, b) VS_2, c) MoS_2 and d) VS_2-MoS_2 mixture cells at 2 A g^{-1}.

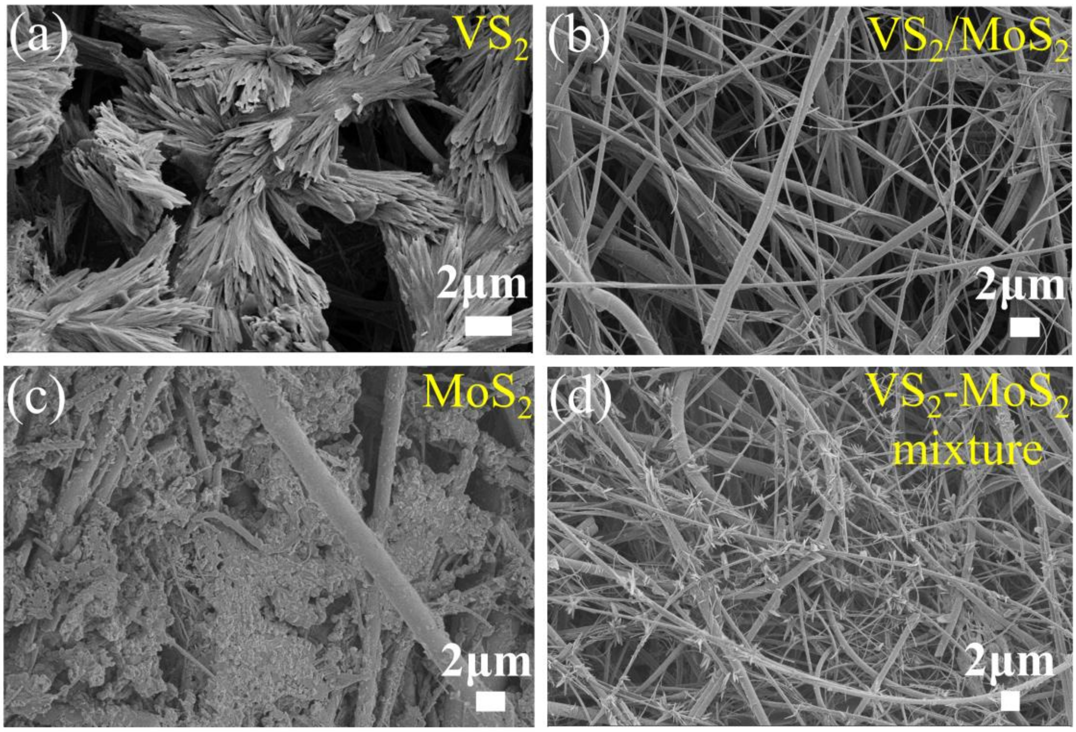

Figure S14. The SEM images of the separators from the spent a) VS_2, b) VS_2/MoS_2, c) MoS_2 and d) VS_2-MoS_2 mixture cells at 2 A g^{-1}.

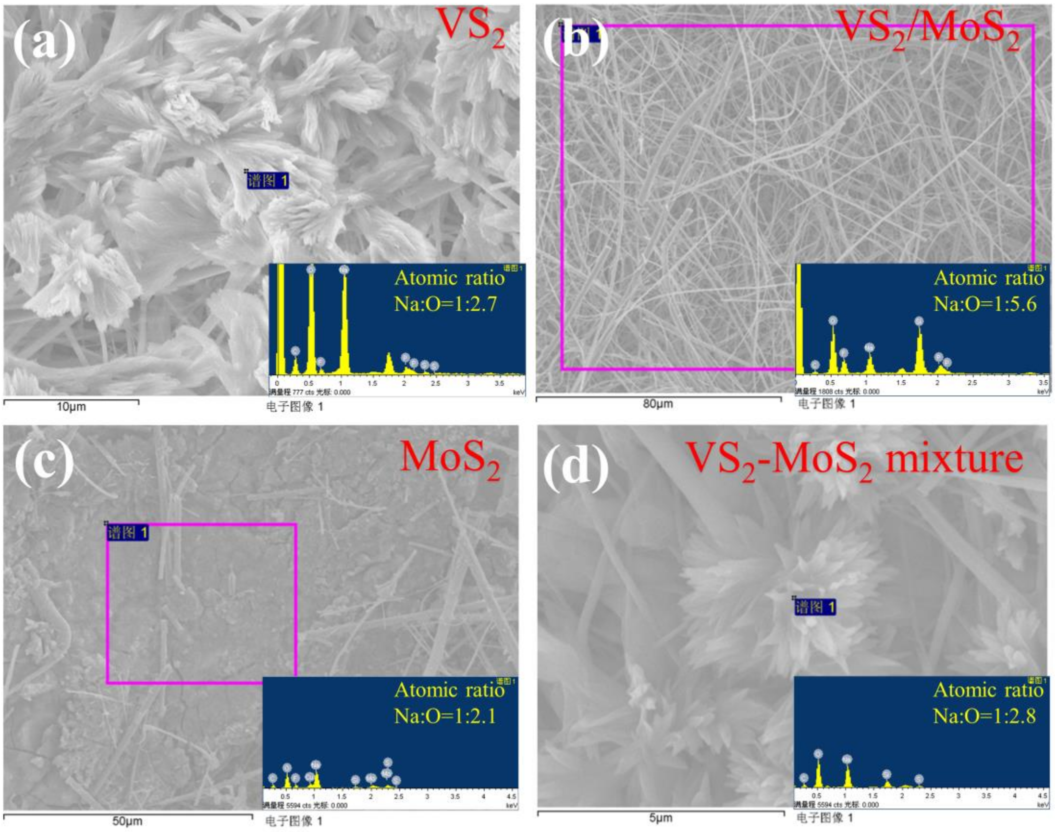

Figure S15. The energy dispersive X-ray spectrum (EDS) results of the spent separator from the a) VS_2, b) VS_2/MoS_2, c) MoS_2 and d) VS_2-MoS_2 mixture cells at 2 A g^{-1}.

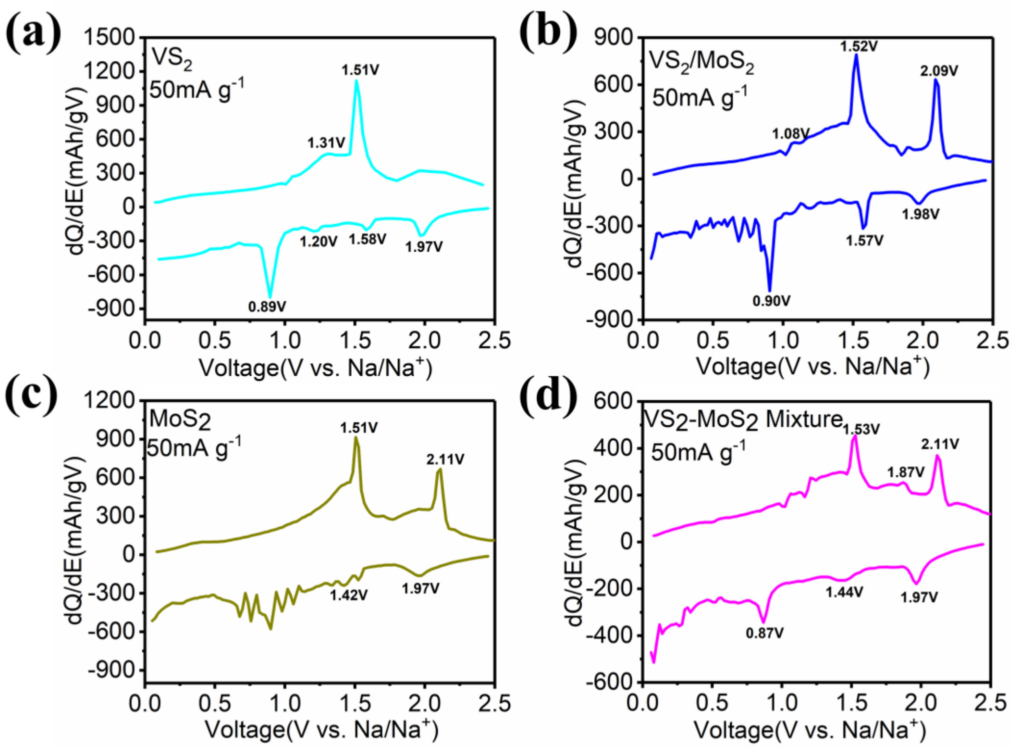

Figure S16. The dQ/dE patterns of a) VS_2, b) VS_2/MoS_2, c) MoS_2 and d) VS_2-MoS_2 mixture electrodes at 50 mA g^{-1}, inset discharge/charge curves at 50 mA g^{-1}.

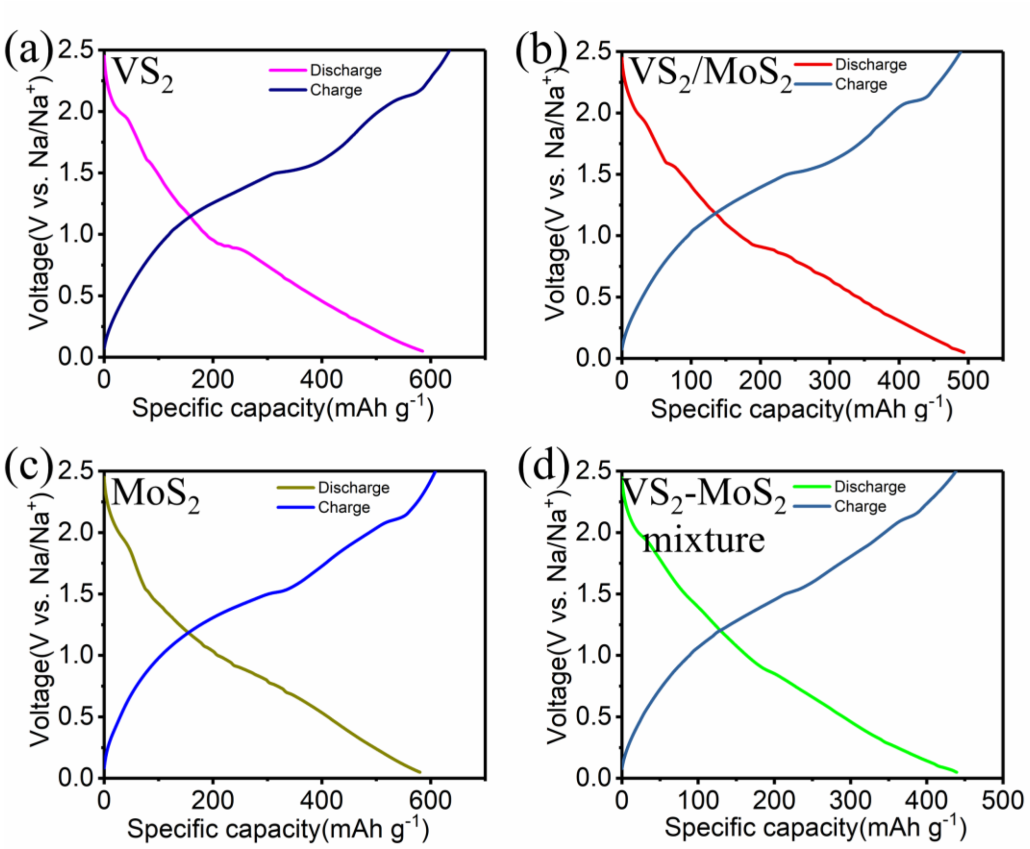

Figure S17. The discharge/charge curves at 50 mA g^{-1} of a) VS_2, b) VS_2/MoS_2, c) MoS_2 and d) VS_2-MoS_2 mixture electrodes.

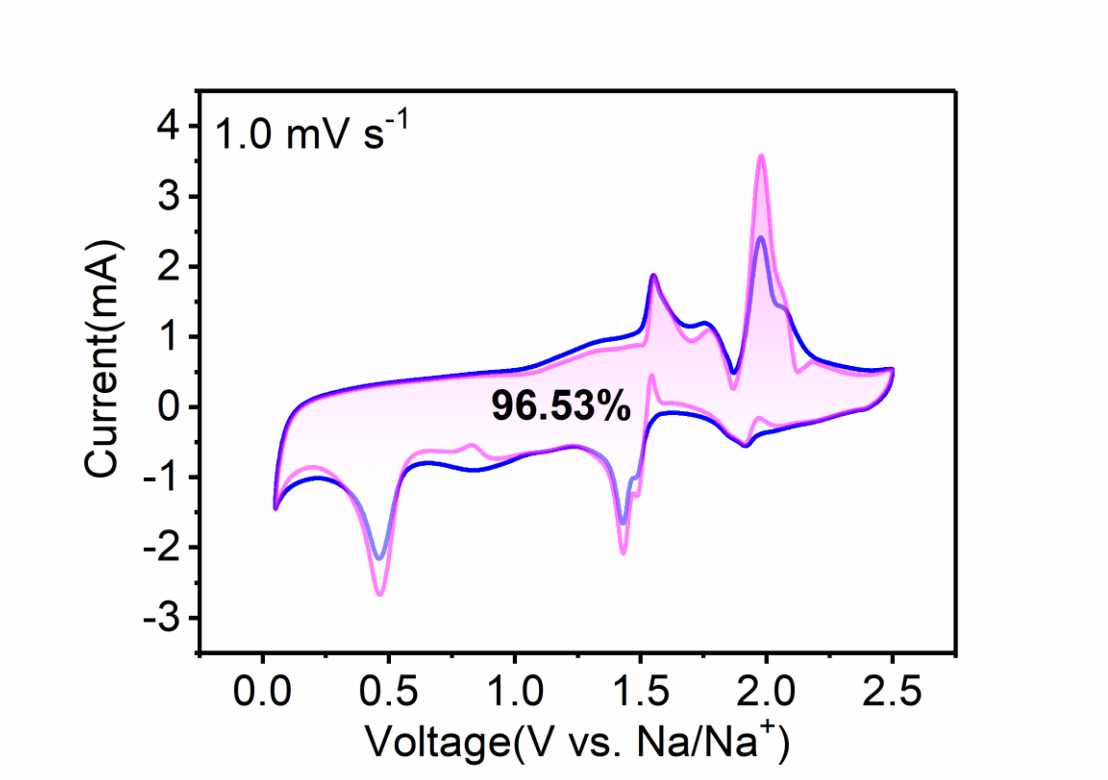

Figure S18. The ratio of diffusion and capacitive contribution to the total capacity at a scan rate of 1 mV s^{-1} for VS_2/MoS_2 electrode.

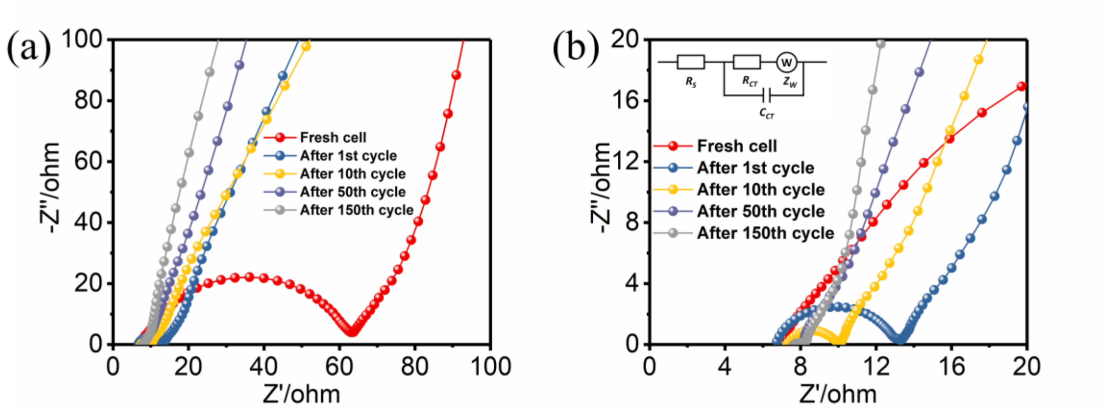

Figure S19. a) Nyquist plots after different cycles for the VS_2/MoS_2 electrode, b) Enlarged view of Nyquist plots with different cycles and equivalent electric circuit (inset).

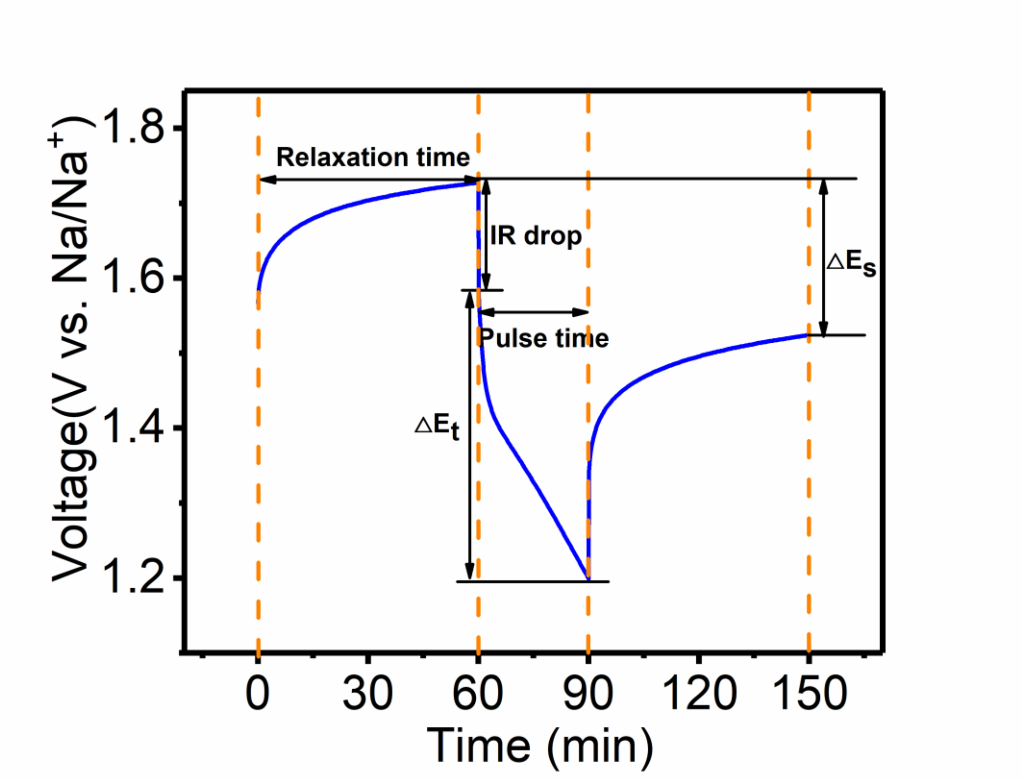

Figure S20. E vs.t curves of VS_2/MoS_2 electrode for a single GITT during discharge process.

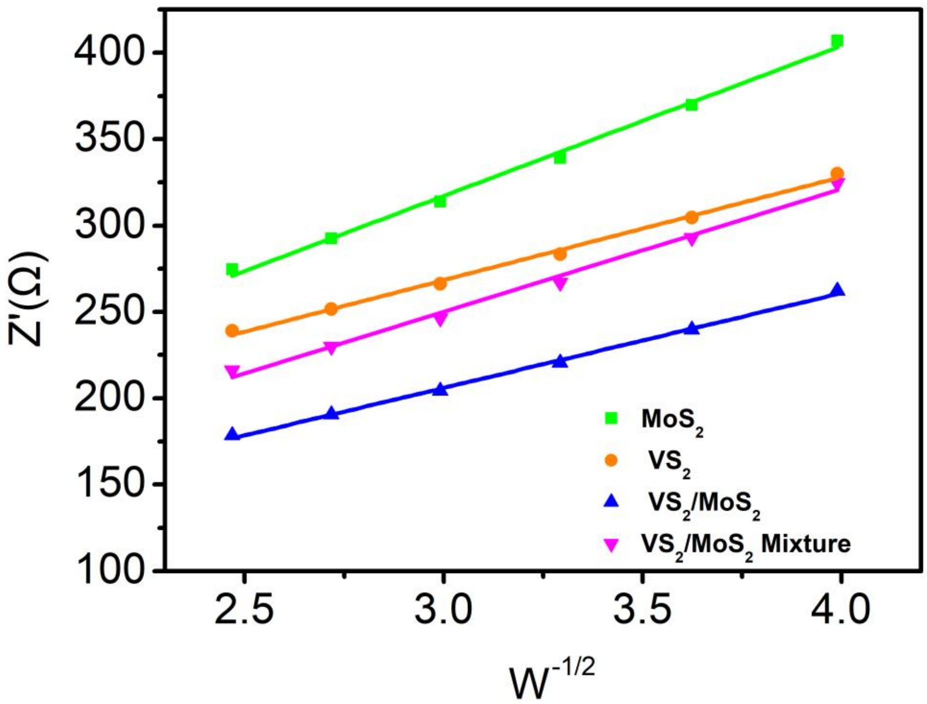

Figure S21. Relationship between Z' and $\omega^{-1/2}$ of VS_2/MoS_2, VS_2, MoS_2 and VS_2-MoS_2

mixture electrodes

According to the EIS results and Equations S2, Supporting Information, the relationship between Z' and $\omega^{-1/2}$ is shown in Figure S15, Supporting Information. σ is the Warburg factor calculated from the slope of the lines between Z' and $\omega^{-1/2}$. And according to Equations S1, Supporting Information, when the R, T, A, F, n and C parameters are constant, the value of D_{Na+} increases with the value of σ decreasing instead.[S2]

Equations S1, S2.

$$D_{Na^+} = \frac{R^2T^2}{2n^4F^4A^2C^2\sigma^2} \qquad \text{(S1)}$$

$$Z' = R_s + R_{ct} + \sigma\omega^{-1/2} \text{(S2)}$$

Where R, T, A, F, n and C represent the gas constant, absolute temperature, electrode surface area, Faraday's constant, molar electron transfer number and molar concentration of Na^+, respectively. And σ is the Warburg factor calculated from the slope of the lines between Z' and $\omega^{-1/2}$.

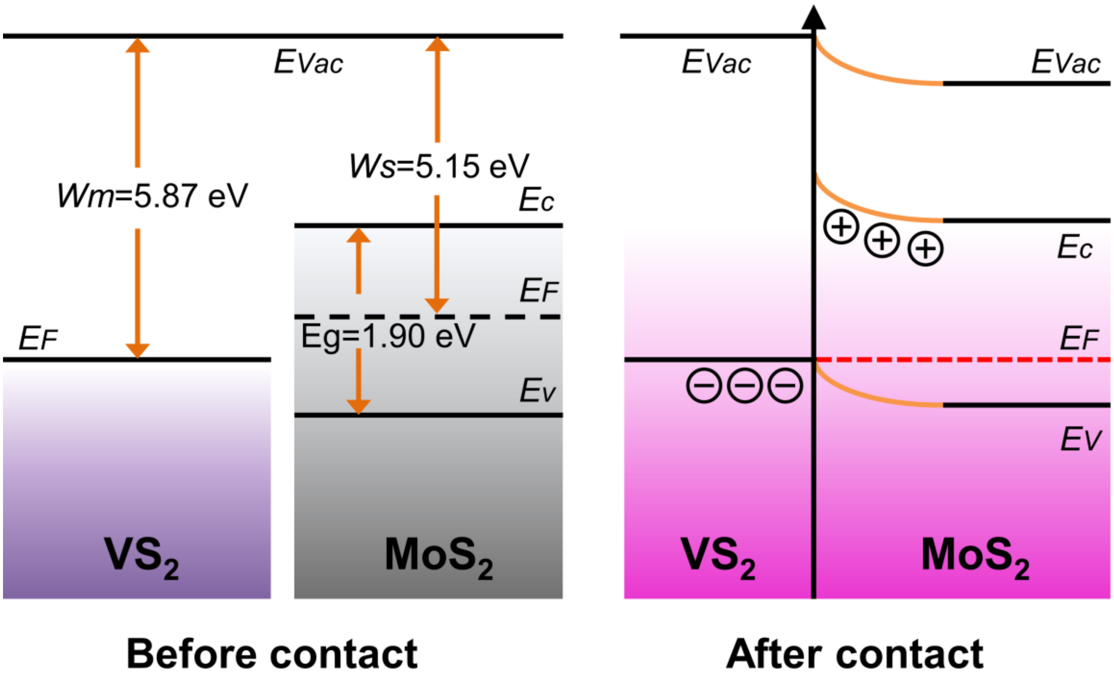

Figure S22. Energy band diagram before and after contact between metal VS_2 and semiconductor MoS_2, where E_{vac}, E_c, E_F, E_v, E_g, and W represent vacuum energy, conduction band, Fermi level, valence band, band gap, and work function, respectively.

Table S1. Comparison of the rate capability and cycling stability of VS_2/MoS_2 with other VS_2 or MoS_2 based anodes for SIBs.

Materials	Specific capacities	Cycle life	Reference
Co_9S_8/MoS_2–CN	438 mAh g^{-1} at 1A g^{-1} 275 mAh g^{-1} at 20 A g^{-1}	421 mAh g^{-1} after 250 cycles at 2A g^{-1}	*J. Mater. Chem. A*, 2018, **6**, 4776-4782.
VS_2 NSA	700 mAh g^{-1} at 0.1A g^{-1} 400 mAh g^{-1} at 2 A g^{-1}	≈500 mAh g^{-1} after 200 cycles at 1A g^{-1}	*Adv. Mater.*, 2017, **29**, 1702061.
ce-V_5S_8–C	616 mAh g^{-1} at 0.5A g^{-1} 344 mAh g^{-1} at 10 A g^{-1}	496 mAh g^{-1} after 500 cycles at 1A g^{-1}	*Energy Environ. Sci.*, 2017, **10**, 107-113.
$VMoS_2$-43	548.1 mAh g^{-1} at 0.1 A g^{-1} 305.6 mAh g^{-1} at 10 A g^{-1}	451.6 mAh g^{-1} after 800 cycles at 2A g^{-1}	*Chem. Eng. J.*, 2021, **417**, 128107.
c-VS_2@VOOH	424 mAh g^{-1} at 0.1A g^{-1} 113 mAh g^{-1} at 5A	330 mAh g^{-1} after 150 cycles at 0.2A g^{-1}	*J. Mater. Chem. A*, 2017, **5**, 20217-

	g^{-1}		20227.
BD-MoS_2	354 mAh g^{-1} at 0.5A g^{-1} 262 mAh g^{-1} at 5 A g^{-1}	350 mAh g^{-1} after 1000 cycles at 2A g^{-1}	*Small*, 2019, **15**, e1805405.
Nb_2CTx@MoS_2@C	530 mAh g^{-1} at 0.1A g^{-1} 454 mAh g^{-1} at 5A g^{-1}	403 mAh g^{-1} after 2000 cycles at 1A g^{-1}	*ACS Nano*, 2021, **15**, 7439-7450.
MoS_2/G	432 mAh g^{-1} at 0.1A g^{-1} 324 mAh g^{-1} at 10A g^{-1}	421 mAh g^{-1} after 250 cycles at 0.3A g^{-1}	*Adv. Energy Mater.*, 2017, **8**, 1702383.
Fe_9S_{10}@MoS_2@C	443 mAh g^{-1} at 0.5A g^{-1} 197 mAh g^{-1} at 30 A g^{-1}	355 mAh g^{-1} after 1000 cycles at 2A g^{-1}	*Energy Storage Mater.*, 2020, **24**, 208-219.
VS_2/MoS_2	781.9 mAh g^{-1} at 0.5A g^{-1} 644.0 mAh g^{-1} at 10	454.5 mAh g^{-1} after 1000 cycles at 2A g^{-1}	This study

A g^{-1}

Table S2. Fitting results of EIS for various samples with the proposed equivalent circuit.

Samples	**R_s(Ω)**	**R_{ct}(Ω)**
VS_2	**1.306**	**87.06**
MoS_2	**6.091**	**135.5**
VS_2-MoS_2 mixture	**5.824**	**104.6**
VS_2/MoS_2	**5.36**	**66.37**

Rs represents the series resistance; Rct indicates the charge-transfer resistance and CPE expresses the constant phase element.

Table S3. Simulated impendence parameters (Rs and Rct) of VS_2/MoS_2 electrode.

Cycle number	**R_s(Ω)**	**R_{ct}(Ω)**
Fresh cell	**7.687**	**56.41**
After 1st cycle	**6.942**	**5.685**
After 10th cycle	**7.524**	**2.208**
After 50th cycle	**7.727**	**0.207**
After 150th cycle	**7.771**	**0.232**

References:

S1 X. Yue, J. Wang, A. M. Patil, X. An, Z. Xie, X. Hao, Z. Jiang, A. Abudula and G. Guan, *Chem. Eng. J.*, 2021, **417**, 128107.

S2 D. Wang, L. Cao, D. Luo, R. Gao, H. Li, D. Wang, G. Sun, Z. Zhao, N. Li, Y. Zhang,

F. Du, M. Feng and Z. Chen, *Nano Energy*, 2021, **87**, 106185.